# Double anomalous peak in the heat capacity just below the triple point of saturated $e$-H$_2$ with FeO(OH) [1]

T. Nakano[2], W. Tew[3], O. Tamura[2] and H. Sakurai[2]

[2] National Metrology Institute of Japan, AIST Central 3, Tsukuba, Ibaraki 305-8563, Japan

[3] Process Measurements Division, National Institute of Standards and Technology

100 Bureau Drive, MS 8363,Gaithersburg, MD 20899-8363, U.S.A.

[4] E-mail; tnt@ni.aist.go.jp

**ABSTRACT**

Heat capacity of e-$H_2$ with podwer of FeO(OH) used as a catalyst for ortho-para equilibration has been investigated using sealed cells fabricated at NIST and at NMIJ. An anomalous double peak has been observed in their heat capacities at temperatures just below the triple point independent of sources of $H_2$ and FeO(OH) and designs of sealed cells. The supercooling behavior has been observed not only at the triple point but also at each anomalous peak owing to a possible phase separation of solid hydrogen with a lower melting temperature due to influence of the catalyst. The reduction of the amount of catalyst suppresses the size of the anomaly and allows one to obtain more reliable melting curves for e-$H_2$.

# 1. INTRODUCTION

Molecular hydrogen ($H_2$) has two isomers, ortho- and para-hydrogen, which differ in the nuclear spin arrangement. Since the triple point temperatures of $H_2$ is dependent on the composition of these isomers, the triple point of nuclear-spin-equilibrated $H_2$ (e-$H_2$) is used as one of the defining fixed points for the International Temperature Scale of 1990 (ITS-90) [1]. Although the composition of the isomers at a thermal equilibrium state is a function of temperature, the equilibrium is only slowly established by changing temperature [2]. So, it is traditionally recommended to use a large amount of catalyst to realize the triple point of e-$H_2$ for the purpose of suppression of the uncertainty due to their non-equilibration [3].

However, it has been recently confirmed that there is a problem for the triple point of e-$H_2$ when a large amount of ferric oxy-hydroxide (FeO(OH)) is used as the catalyst; a large anomalous increase exists in the heat capacity at temperatures just below the triple point [2, 4-7], and the anomalies markedly influence the shape of the melting plateau and the triple point temperature [4-8]. Furthermore, a very recent report showed an anomalous double peak in the heat capacity just below the triple point using a sealed cell containing 89.7 mmol of $H_2$ with 0.53 g of powder of FeO(OH) [7]. The reduction of the amount of FeO(OH) suppresses the anomalies and makes the double peak behavior unclear [7]. Clarification of the detailed behavior of anomalies in the heat capacity has been expected to give a clue to understand its origin and a best way to realize the triple point temperature of e-$H_2$ at highest-level accuracy.

In this study, the heat capacity of e-$H_2$ with powder of FeO(OH) used as the catalyst was examined at temperatures around the triple point using sealed cells fabricated at NIST and at NMIJ. Although these institutes used different sources of $H_2$ and FeO(OH)

and different designs of sealed cells, the anomalous double peak has been evidently observed at both institutes in their heat capacities at temperatures just below the triple point. We also tried to check the detailed behavior of the double peak in the heat capacity using NMIJ cells, and evidently confirmed that the double peak occurs in the heat capacity regardless of the amount of FeO(OH). The supercooling behavior also appears not only at the triple point but also at each anomalous peak, implying that the anomalous peaks could be caused by a phase separation within the solid hydrogen. The phase of the solid in close physical proximity to the catalyst appears to have a lower melting temperature due to magnetic interactions between the powder of FeO(OH) and that portion of solid $H_2$.

## 2. MEASUREMENTS

The designs of sealed cells fabricated at NIST and NMIJ are shown in Figs. 1 (a) and 1 (b), respectively. The NIST cell consists of stainless steel cylinder and copper insert with three thermometer wells. Its inner volume is about 40 cm$^3$ and a confined space for liquid and/or solid sample is about 3 cm$^3$. On the other hand, the NMIJ cell consists of only copper and its insert has one thermometer well. Its inner volume is about 35 cm$^3$ and a confined space is about 2 cm$^3$. The detailed designs of these cells including gas filling systems and related techniques have been described elsewhere. [7, 9-11].

In this study, we used two NIST cells and three NMIJ cells. The NIST cells, 212 and 213, use $H_2$ obtained from MG Industries, Malvern PA, USA. The NMIJ cells, H-1, H-2, and H-5 use $H_2$ gas from Nippon Sanso, Japan. The nominal chemical purity of $H_2$ of all sources for both institutes is better than 99.9999 %. A summary of the various cells contents, including isotopic composition of the gas , is given in Table 1.

Measurements of heat capacity around the triple point for e-$H_2$ sealed cells fabricated at NIST and at NMIJ have been done by the adiabatic calorimeters manufactured at respective institutes. These apparatuses used at NIST and at NMIJ and the detailed measurement procedures have been reported elsewhere. [7, 9-11].

## 3. RESULTS AND DISSCUSSION

3.1 Double anomalous peak in heat capacity of e-$H_2$ with powder of FeO(OH)

Figures 2 (a) and 2 (b) show the heat capacities of e-$H_2$ cells fabricated at NIST (213) and at NMIJ (H-1, H-2 and H-5) near the triple point, respectively. An anomalous double extra peak, other than a divergence due to the triple point, is evidently observed for these cells at temperatures just below the tripe point. Hereafter, each peak is referred to as an anomaly. The 1st anomaly, which is nearer to the triple point, is much larger than the 2nd one. Both anomalies are suppressed by reducing the amount of the catalyst, as seen in Fig 2 (b). In the former report [7], existence of 2nd anomalies for H-2 and H-5 cells were unclear. But, a 2nd anomaly can be clearly observed even for H-5 cell including only 0.015 g of FeO(OH) by reducing the size of each heat pulse down to 0.005 J in the present study, as seen in the inset of Fig. 2 (b). Recently, Fellmuth et al. also confirmed the anomalous double peak in the heat capacity of e-$H_2$ using some of the same sealed cells [12]. These results indicate that the double peak behavior in the heat capacity of e-$H_2$ with powder of FeO(OH) is a universal property independent of $H_2$ sources, FeO(OH) sources, FeO(OH) amounts, and sealed-cell designs.

Figure 3 shows the enthalpy gain due to the anomalies and the triple point transition of H-1 cell obtained from integration of the excess of heat capacity over the normal heat capacity in the same way reported in Ref.7. The inset of Fig. 3 shows the dependence on the amount of FeO(OH) of the enthalpy gain due to the triple point transition ($\Delta H_0$), 1st anomaly ($\Delta H_1$) and 2nd anomaly ($\Delta H_2$). The sizes of $\Delta H_1$ and $\Delta H_2$ increase in proportion to the amount of the catalyst. This correlation strongly indicates that the

catalyst causes the both anomalies on heat capacity, as reported previously [2, 4-8].

The total enthalpy gain due to both of the anomalies and the triple point transition, $\Delta H_0$ + $\Delta H_1$ + $\Delta H_2$, is about 10 J and accords with the total heat of fusion expected from the amount of hydrogen in each cell, as reported in Ref. 7.  We also confirmed this accordance not only for H-1, H-2 and H-5 cells but also for 213 cell.  This strongly suggests that the anomalous double peak is related to the melting of a part of the solid hydrogen, as reported previously [7].

3.2 Heat capacity of e-$H_2$ with powder of FeO(OH) in its supercooling state

Figure 4 shows the freezing curve of $H_2$ observed using H-1 cell.  The cooling power was about 60 mW.  First, the temperature decreases down to about 30 mK below the triple point temperature because of supercooling.  Next, the temperature jumps up to the triple point temperature and keeps it for about 2 hours because of solidification of $H_2$ at the triple point.  Later, temperature starts to decrease and shows a "shoulder" behavior around temperatures where the anomalies in the heat capacity have been observed. Finally, the temperature decreases steeply. To check the heat capacity in the supercooling state, the adiabatic calorimetry was started around the temperature $T_o$ in Fig 4.  To investigate the origin of the shoulder behavior, we also stopped the cooling at temperatures around the shoulder, $T_1$ and $T_2$ in Fig. 4, and then started measurements of heat capacity for H-1 cell.

Figure 5 shows the heat capacity of H-1 cell, measurements of which were started at a temperature $T_0$, $T_1$ and $T_2$ in Fig. 3.  The heat capacity of RUN $T_o$, namely the heat capacity in the supercooling state, shows almost constant behavior around the triple point without any anomaly at those temperatures, where the 1st anomaly was observed. This means that the anomalies will not occur without solid hydrogen.   It is consistent

with the above suggestion that the anomalies are related to the melting of a part of the solid hydrogen.

As seen in Fig. 5, the heat capacity of RUN $T_1$ increases with increasing temperatures without showing 1st anomaly and agrees with the divergent part of heat capacity due to the triple point at higher temperatures.   This strongly suggests that the supercooling of the 1st anomaly phase will occur independently of the normal transition at the triple point.   Similar behavior was also observed in RUN $T_2$ at temperatures around 2nd anomaly, as seen in the inset of Fig. 5.   These results imply that solid $H_2$ will mainly separate into three phases with the different melting temperatures. The shoulder behavior in Fig. 4 will be caused by the solidification into the different solid phases, which cause 1st and 2nd anomalies in the heat capacity.

Figure 6 shows the schematic view of solid $H_2$ with FeO(OH) filled in a cell.   The presence of the catalyst particles naturally separates the solid $H_2$ into two volumes within the cell; one volume contains the solid phase coexisting with the catalyst FeO(OH), and the other volume contains the solid phase separated from the catalyst.   As mentioned above, the size of anomalies in the heat capacity shows a linear dependence on the amount of the catalyst [7, 10].   So, the anomalies will come from the solid phase coexisting with the catalyst.

The catalysts being used for these sealed-cells are prepared by precipitation from hydrous gels.[14] This process creates a very high porosity and hence a high active surface area when the gel is dried into the powder. An additional vacuum activation process is carried out either within the cells prior to filling with $H_2$ or in a seperate vacuum-reactor mainly to remove any remaining adsorbed $H_2O$ and $N_2$ from these

active surfaces. During activation powder particles of FeO(OH) tend to adhere each other and easily become small clusters. Such a cluster will create additional porosity. Probably, a part of hydrogen confined within such a porous catalyst will be followed by a depression of the melting temperature and become solid phases causing the anomalies in the heat capacity at temperatures just below the triple point. It is possible that differences in the activation proceedures used at NMIJ and NIST resulted in slight differences in the final chemical form of the catalyst, including the possibility of some catalyst transforming to anhydrous $Fe_2O_3$ .

Similar phenomena have been actually observed in other substances. For example, a depression of the melting temperature was observed for solid indium confined in iron [13]: its melting temperature is reduced with decreasing the radius of the confined space in iron, which is explained by the interfacial energies between iron and solid (or liquid) indium. As mentioned above, the double peak is observed in the heat capacity of e-$H_2$ with powder of FeO(OH). The reason of the appearance of the double peak is not clear from this study alone, but it may come from the existence of different size scales of confined spaces in the porous catalyst. Or it may be possible that the second (lower temperature) anomaly is caused by a solid-solid transition for that portion of the $H_2$ within the pores of the catalyst particles.

3.3 Melting curves of e-$H_2$ at the triple point

The melting curves for H-1, H-2 and H-5 cells are shown in Fig. 7. The data obtained in heat capacity measurements are plotted against the inverse of melted fraction,$1/F$. To evaluate $F$, $\Delta H_0$ was used as the total heat of fusion. In Fig. 7, the melting curves reported in Ref. 7 are also shown. In Ref. 7, the melted fraction $F$ was evaluated by using $\Delta H_0 + \Delta H_1 + \Delta H_2$ as the total heat of fusion; that is, the melting curves reported in Ref. 7 included the contribution of the other phases of solid $H_2$ with lower melting

temperatures due to the influence of the catalyst.

As seen in Fig. 7, the width of the melting curves of H-1 and H-2 cells become narrow within about 0.2 mK in the wide region of $1/F$ up to $1/F = 10$ by removing the contribution of $\Delta H_1$ and $\Delta H_2$. On the other hand, both melting curves for H-5 obtained in the present study and in Ref. 7 show the same linear dependence on $1/F$. This is because the contributions of $\Delta H_1$ and $\Delta H_2$ for H-5 cell are very small owing to the reduction of the amount of the catalyst.

The melting curves of H-1 and H-2 cells show almost the same value of H-5 cell at $1/F$ <2, but they deviate downward from the linear dependence of H-5 cell with increasing $1/F$ at $1/F > 2$ although the contribution of $\Delta H_1$ and $\Delta H_2$ were removed. Probably, this suggests that influence of the catalyst causing the suppression of the melting temperature will reach outside of the catalyst when a large amount of the catalyst was used.

Figure 8 shows melting curves of 212 and 213 cells. The melted fraction $F$ was evaluated by using $\Delta H_0 + \Delta H_1 + \Delta H_2$ as the total heat of fusion. Since both cells include the same ratio of the amounts of $H_2$ and FeO(OH), it is expected to observe almost the same behavior of the melting curves. However, suppression of the melting temperature due to the catalyst is larger for 213 cell than that for 212 cell at higher $1/F$ region, as shown in Fig. 8.

If the correlation length of the influence of the catalyst exists outside of catalyst as the above suggestion, the effect will depend on the amount of hydrogen even if the same ratio of the amounts of $H_2$ and FeO(OH) is included in each cell; the influence of the catalyst will become larger in the case of the cell including a smaller amount of $H_2$. This is consistent with the measurement result; the influence on the melting curve for

213 cell including a smaller amount of hydrogen is larger than that for 212 cell.

## CONCLUSION

The heat capacity of e-$H_2$ with powder of FeO(OH) used as the catalyst for ortho-para equilibration has been examined using sealed cells fabricated at NIST and at NMIJ. An anomalous double peak appears in their heat capacities at temperatures just below the triple point independently of $H_2$ sources, FeO(OH) sources, their amounts and designs of sealed cells. The supercooling behavior has been observed not only at the triple point but also at each anomalous peak, implying that the anomalous double peak will be caused by localized pre-melting or other endothermic transformations of the solid hydrogen due to magnetic or other interactions between the catalyst and $H_2$. The reduction of the amount of catalyst suppresses the influence of the catalyst and allows one to obtain more reliable melting curves for e-$H_2$.

## REFERENCES

[1]   H. Preston-Thomas, *Metrologia* **27**, 1990, pp. 3-10, *ibid.*, p. 107 (erratum).

[2]   H. Sakurai, *T. SICE,* **34**, pp. 1153-1158, (1998).

[3]   *Supplementary Information for the International Temperature Scale of 1990*, BIPM, 1990.

[4]   H. Sakurai, *Proceedings of TEMPMEKO 2001*, Berlin: VDE VERLAG GMBH, 2002, pp. 411-416.

[5]   H. Sakurai, in: *Temperature, its Measurement and Control in Science and Industry,* **Vol. 7**, D. C. Ripple, ed., American Institute of Physics,  (to be published). (2002).

[6]   B. Fellmuth, *et. a.l*, *Proceedings of TEMPMEKO 2001*, Berlin; VDE Verlag GmbH, 2002, pp. 403-405.

[7] T. Nakano, O. Tamura and H. Sakurai, in: *Temperature, its Measurement and Control in Science and Industry,* **Vol. 7**, D. C. Ripple, ed., American Institute of Physics,  (to be published). (2003).

[8] A. G. Steele, *Proceedings of TEMPMEKO 2001*, Berlin; VDE Verlag GmbH, 2002, pp. 417-422.

[9] W. L. Tew, *Proceedings of TEMPMEKO '96*, Torino; Levrotto & Bella, 1997, pp. 81-86.

[10] T. Nakano, O. Tamura and H. Sakurai, *T. SICE* **38**, 2002, pp. 947-951.

[11] C. W. Meyer and W. L. Tew, , in: *Temperature, its Measurement and Control in Science and Industry,* **Vol. 7**, D. C. Ripple, ed., American Institute of Physics, (to be published). (2003).

[12] B. Fellmuth, *et al.*. (to be submitted to) *Metrologia,* (2003).

[13] T. Ohashi, K. Kuroda and H. Saka, *Phil. Mag. B* **65**, 1992, pp. 1041-1052.

[14] P. L. Barrick, L. F. Brown, H. L. Hutchinson, and R. L. Cruse*, Adv. Cryo. Engin.*, **10A**, 181-189, (1965).

Table 1. Sealed-Cell gas and catalyst content summary.

| Cell ID | Institute | $H_2$ / mmol | $m_{Cat}$ / g | Catalyst Mesh | D/H $\mu$mol/mol |
|---------|-----------|--------------|---------------|---------------|------------------|
| H-1 | NMIJ | 85.5 | 0.53 | <200 | 27.2 |
| H-2 | NMIJ | 89.7 | 0.12 | <200 | 27.2 |
| H-5 | NMIJ | 89.7 | 0.015 | <200 | 27.2 |
| 212 | NIST | 68 | 0.20 | 30-50 | 29.1 |
| 213 | NIST | 59 | 0.17 | 30-50 | 29.1 |

**Figure Captions**

**Fig. 1.** Sealed cells: (a) fabricated at NIST [9] and (b) that fabricated at NMIJ [7].

**Fig. 2.** Heat capacities around the triple point observed by using: (a) NIST cell no. 213 at two different heating powers and (b) H-1, H-2 and H-5 cells fabricated at NMIJ. The inset is an enlarged figure of the heat capacity of H-5 around 2nd anomaly.

**Fig. 3.** Enthalpy gain due to the anomalies and the triple point transition of H-1 cell obtained from integration of the excess of heat capacity over the normal heat capacity. The inset shows the dependence on the amount of catalyst of the enthalpy gains due to the triple point transition ($\Delta H_0$), 1st anomaly ($\Delta H_1$) and 2nd anomaly ($\Delta H_2$).

**Fig. 4.** Freezing curve observed by using H-1.

**Fig. 5.** Heat capacity of H-1 measurements of which were started at a temperature $T_0$, $T_1$ and $T_2$ in Fig. 3.

**Fig. 6.** Schematic view of solid $H_2$ with FeO(OH) filled in a cell.

**Fig. 7.** Melting curves obtained by using H-1, H-2 and H-5. Dashed, dashed–and-dotted and solid lines are melting curves reported in Ref. 7 for H-1, H-2 and H-5, respectively.

**Fig. 8.** Melting curves obtained by using NIST cells 212 and 213 under repeated melting runs.

(a)
Pinch Weld
Ballast Volume
Helical Exchange Fins
Sample Volume
Thermometer Wells

(b)
Locking bolt
Copper plug
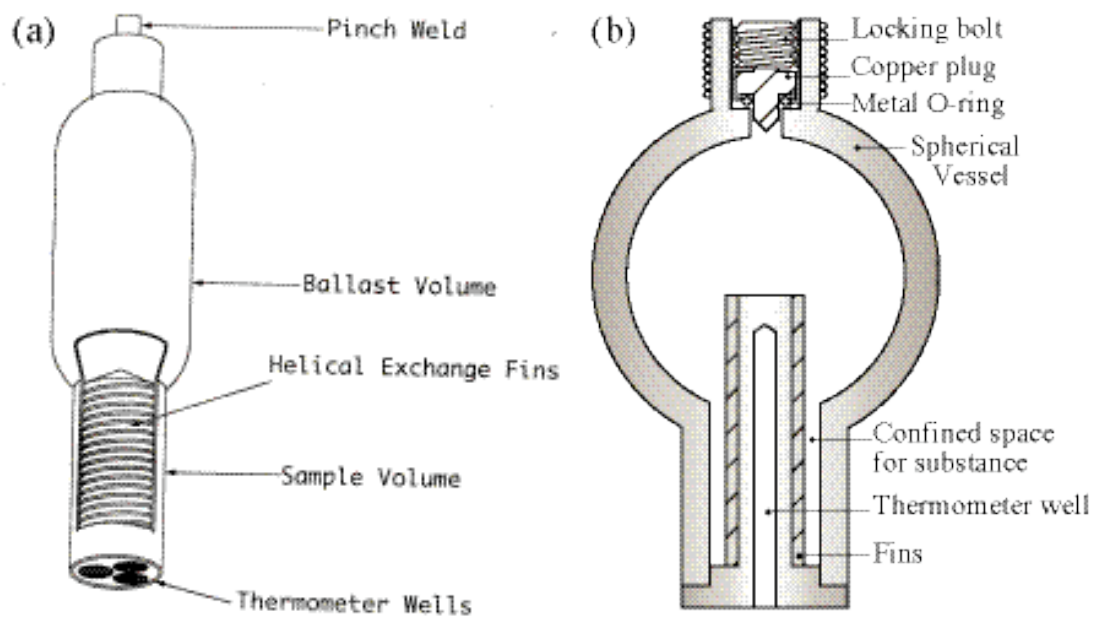Metal O-ring
Spherical Vessel
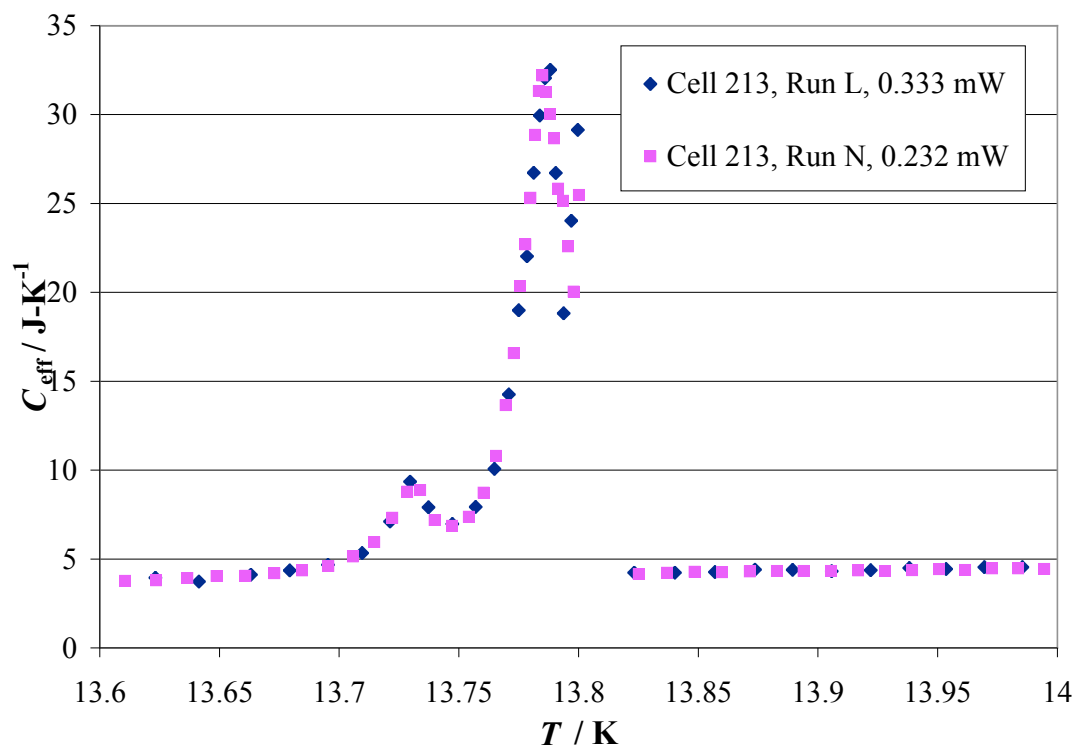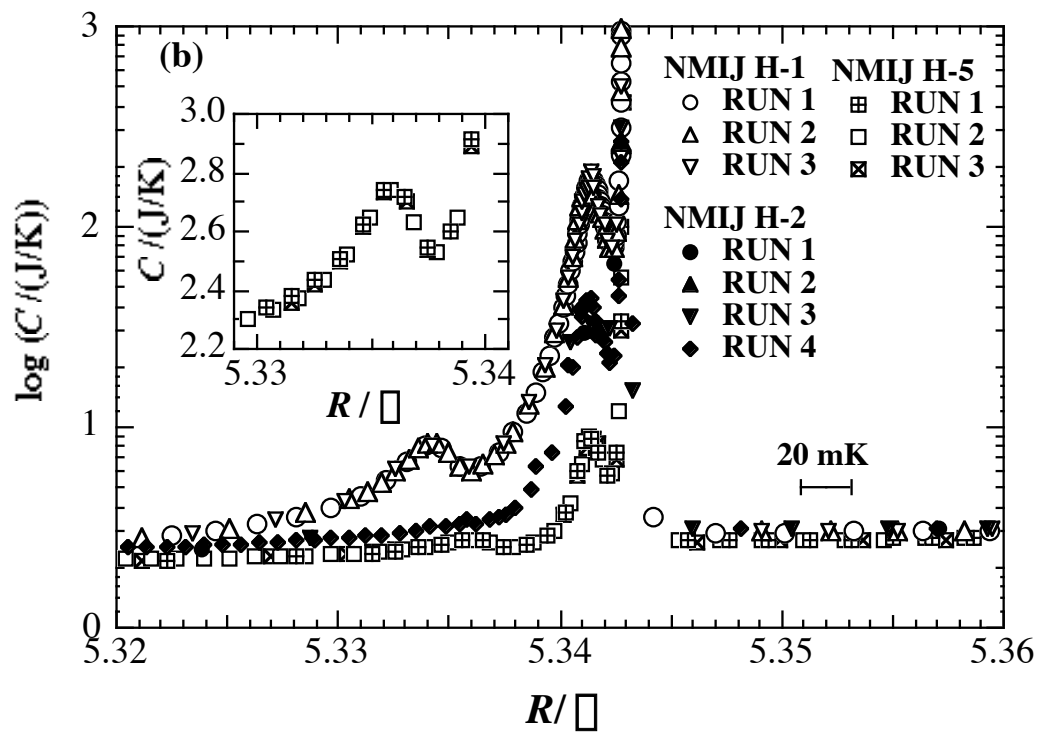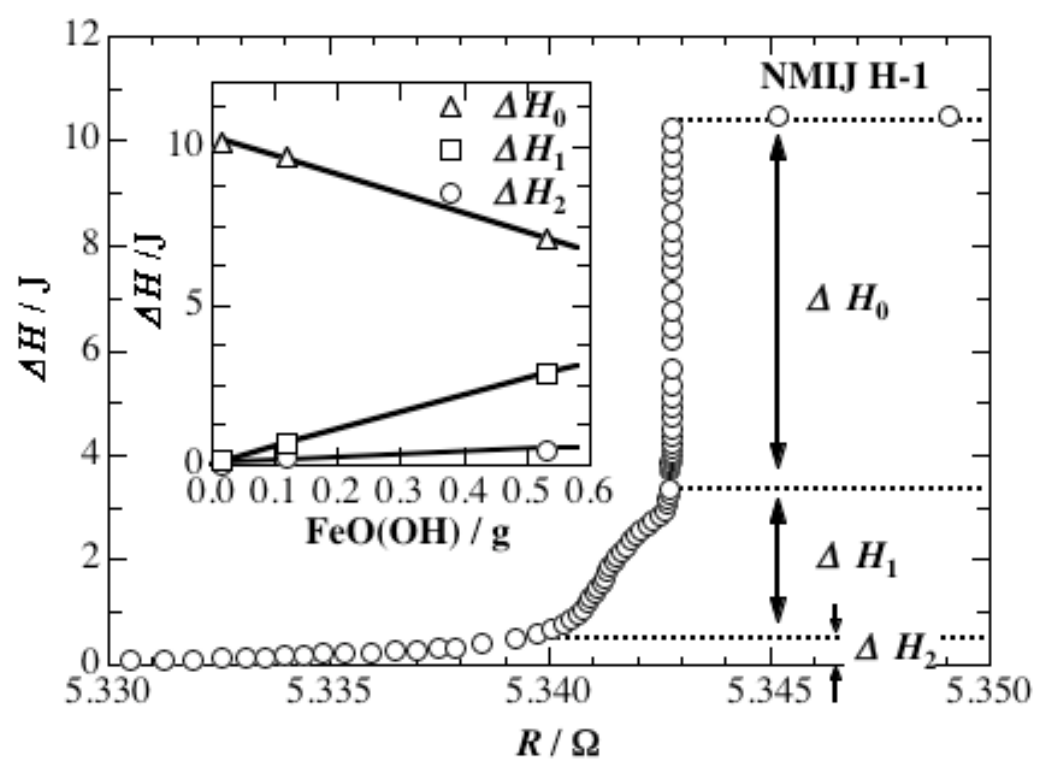Confined space for substance
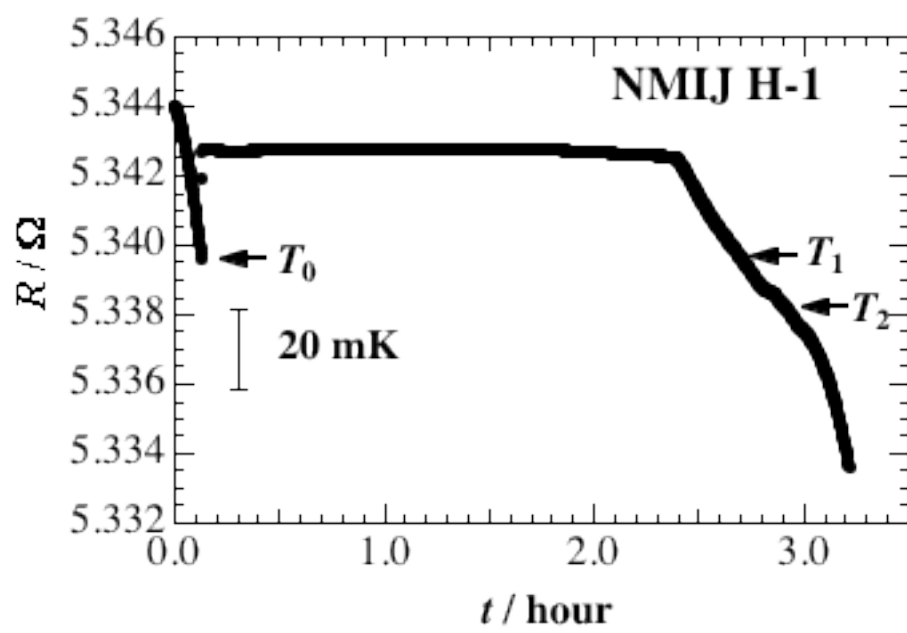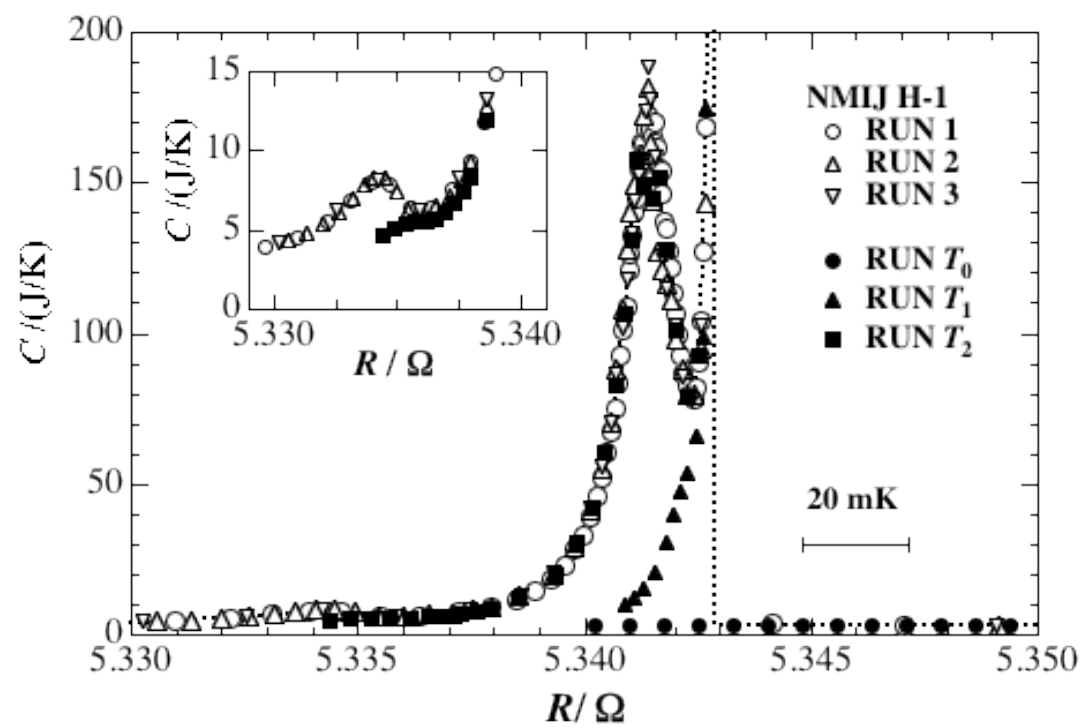Thermometer well
Fins

Fig. 1 (a) and (b)

Fig 2 (a)

Fig. 2 (b).

Fig. 3.

Fig. 4.

Fig. 5.

Fig. 6.

Fig. 7.

Fig. 8.